

Spreading of correlations in Markovian open quantum systems

Vincenzo Alba¹ and Federico Carollo²

¹*Institute for Theoretical Physics, Universiteit van Amsterdam,
Science Park 904, Postbus 94485, 1098 XH Amsterdam, The Netherlands*

²*Institut für Theoretische Physik, Universität Tübingen,
Auf der Morgenstelle 14, 72076 Tübingen, Germany*

Understanding the spreading of quantum correlations in out-of-equilibrium many-body systems is one of the major challenges in physics. For *isolated* systems, a hydrodynamic theory explains the origin and spreading of entanglement via the propagation of quasi-particle pairs. However, when systems interact with their surrounding much less has been established. Here we show that the quasi-particle picture remains valid for open quantum systems: while information is still spread by quasiparticles, the environment modifies their correlation and introduces incoherent and mixing effects. For free fermions with gain/loss dissipation we provide formulae fully describing incoherent and quasiparticle contributions in the spreading of entropy and mutual information. Importantly, the latter is not affected by incoherent correlations. The mutual information is exponentially damped at short times and eventually vanishes signalling the onset of a classical limit. The behaviour of the logarithmic negativity is similar and this scenario is common to other dissipations. For weak dissipation, the presence of quasiparticles underlies remarkable scaling behaviors.

Introduction.— Recent years have witnessed tremendous breakthroughs in understanding the origin and spreading of entanglement in out-of-equilibrium many-body systems. In particular, a well-established hydrodynamic picture, predicated on the existence of stable quasiparticles, allows for the description of the entanglement dynamics in integrable systems [1–3]. The unique ability of these systems to transfer quantum correlations can be potentially leveraged in quantum technologies [4] and their implementations in quantum computers are now within reach [5]. Unfortunately, in realistic settings, a coupling with an environment is unavoidable and typically induces a quick decay of quantum coherence.

This loss of quantum information is also the key of the black-hole information paradox [6–8]. Black holes can evaporate by emitting Hawking radiation in a perfectly mixed state. Thus, one is left with the conundrum that an initially pure state (the black hole) gets transformed in a mixed one (radiation) after the black-hole evaporates. As it was pointed out by Page [9, 10], the paradox is apparent after the black hole is half evaporated at $t_{\text{Page}} \approx t_{\text{evap}}/2$. Interestingly, operational schemes to solve this paradox are based on decoherence [11, 12]. Their virtue is that even a small decoherence dramatically reduces the mutual information between the inside and the outside of the black-hole [13], delaying the onset of the paradox to times when the black hole is nearly evaporated, and the semiclassical treatment [6] might break down.

This demonstrates how understanding the fate of entanglement in open quantum systems will have immediate impact on very different branches of physics. Still, modelling quantum information loss, or even sieving genuine quantum coherence from classical correlations, is considered a daunting task. Here, for the first time, we show that these aspects can be understood within the hydrodynamic theory and encapsulated in properties of quasiparticles.

We adopt the framework of Markovian open quan-

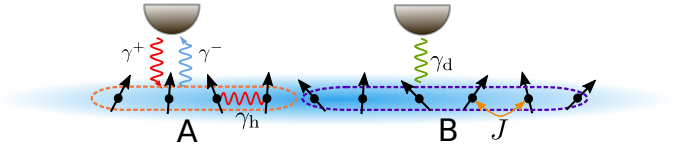


FIG. 1. Sketch of a fermionic open quantum chain. We consider different dissipative effects. Rates γ^\pm are related to fermion creation and annihilation. γ_h and γ_d are, instead, rates for incoherent hopping of fermions and dephasing, respectively. Here the coefficient J represents the amplitude of coherent hopping. The chain is bipartite as $A \cup B$.

tum dynamics [14]. In these settings (weak system-environment coupling and absence of memory effects), the time-evolution of any initial density matrix ρ_0 is generated by the Lindblad master equation $\dot{\rho}_t = \mathcal{L}[\rho_t]$ with the Liouvillian \mathcal{L} being [14]

$$\mathcal{L}[\rho] = -i[H, \rho] + \sum_{\mu} \left(L_{\mu} \rho L_{\mu}^{\dagger} - \frac{1}{2} \{L_{\mu}^{\dagger} L_{\mu}, \rho\} \right). \quad (1)$$

Here $-i[H, \rho]$ describes the coherent evolution under a many-body Hamiltonian H , whereas Lindblad operators L_{μ} effectively account for the presence of an environment.

We consider a fermionic chain with L sites (see Fig. 1) and denote standard creation and annihilation operators as c_m^{\dagger}, c_m for each site. We focus on the XX chain Hamiltonian $H = \sum_{m,n=1}^L h_{mn} c_m^{\dagger} c_n + \text{h.c.}$ with $h_{nm} = J \delta_{|n-m|,1}$. We discuss several sources of dissipation, namely gain/loss, i.e., creation and annihilation of fermions in all sites, incoherent hopping and dephasing. Gain/loss is described by $L_m^+ = \sqrt{\gamma^+} c_m^{\dagger}$ and $L_m^- = \sqrt{\gamma^-} c_m$. A similar Lindbladian has been considered very recently in Ref. 15. Incoherent hopping [16] corresponds to $L_{L,m} = \sqrt{\gamma_h} c_m^{\dagger} c_{m+1}$ and $L_{R,m} = L_{L,m}^{\dagger}$ describing jumps of particles on the left or on the right. Finally, dephasing is modelled by $L_{d,m} = \sqrt{\gamma_d} c_m^{\dagger} c_m$. We study the

dynamics ensuing from the Néel state $|N\rangle \equiv |\uparrow\downarrow\uparrow\cdots\rangle$, although any product state can be treated analogously.

To quantify information spreading we divide the system into two parts, as $A \cup B$ (see Fig. 1). From the reduced density matrix $\rho_{A/B}$ we define the Rényi entropies $S_{A/B}^{(\alpha)} = 1/(1-\alpha) \ln \text{Tr} \rho_{A/B}^\alpha$, with $\alpha \in \mathbb{R}$. The von Neumann entropy is obtained by taking $\alpha \rightarrow 1$ as $S_{A/B} \equiv -\text{Tr} \rho_{A/B} \ln \rho_{A/B}$. The mutual information $I_A^{(\alpha)} = S_{A/B}^{(\alpha)} + S_A^{(\alpha)} - S_{AUB}^{(\alpha)}$ is thus a measure of the total correlation between a A and B . The logarithmic negativity [17–27] is instead a genuine measure of the entanglement. This is obtained from the partial transpose ρ_A^T , with $\langle \varphi_i, \bar{\varphi}_j | \rho_A^T | \varphi'_i, \bar{\varphi}'_j \rangle = \langle \varphi_i, \bar{\varphi}'_j | \rho_A^T | \varphi'_i, \bar{\varphi}_j \rangle$, where $|\varphi_i\rangle$ and $|\bar{\varphi}_i\rangle$ are two orthonormal bases for A and B . For free fermions, $\rho_A^T = (e^{-i\frac{\pi}{4}} O_+ + e^{i\frac{\pi}{4}} O_-)/\sqrt{2}$, with O_\pm two gaussian operators [28]. Thus, ρ_A^T is not gaussian and the computation of the logarithmic negativity is difficult even for free fermions. Recently, an alternative negativity, $\mathcal{E} \equiv \ln \text{Tr} \sqrt{O_+ O_-}$, has been introduced [26]. \mathcal{E} is an entanglement monotone under local operations and classical communication preserving the local fermion-number parity [29] and can be easily computed (see Appendix F).

In out-of-equilibrium integrable systems after a *quantum quench* [30–33], the quasiparticle picture [1–3, 34] allows one to describe the dynamics of the von Neumann entropy [3], the steady-state Rényi entropies [35–38], and the mutual information [34, 39], also for quenches from inhomogeneous initial states [40–43]. Remarkably, it has been shown that $\mathcal{E} = I_A^{(1/2)}/2$ [44], then verified in holographic calculations [45], and observed in systems with defects [46]. In the quasiparticle picture the initial state acts as a source of pairs (or multiplets [47–49]) of entangled quasiparticles. As they propagate, they entangle larger and larger portions of the system. The entanglement entropy $S(t)$ is proportional to the number of entangled pairs that at time t are shared between A and B . For generic integrable systems, both interacting and free, the local steady-state physics is described by a Generalized Gibbs Ensemble [30–33] (GGE). Remarkably, the entanglement content of the quasiparticles is the GGE thermodynamic entropy, whereas the quasiparticles velocity is calculated from the excitations above the GGE macrostate [3]. How does such scenario change in open quantum systems? Here we show that for open quantum free-fermionic systems subject to linear [50] diagonal dissipation the information dynamics is indeed captured by a modified quasiparticle picture. This allows for a complete analytical description of $S^{(\alpha)}$ and $I_A^{(\alpha)}$. Crucially, the environment affects the correlation content of the quasiparticles, and creates also classical contributions. Interestingly, the mutual information is only sensitive to the contribution from quasi-particles, and its dynamics closely reflects that of the negativity, despite not being a proper entanglement measure. For weak dissipation we reveal the remarkable scaling behavior

$$\gamma S^{(\alpha)} = f_\alpha(\gamma t, \gamma \ell), \quad \gamma \mathcal{E} = g(\gamma t, \gamma \ell), \quad (2)$$

with $f_\alpha(x)$ and $g(x)$ two scaling functions, and γ the

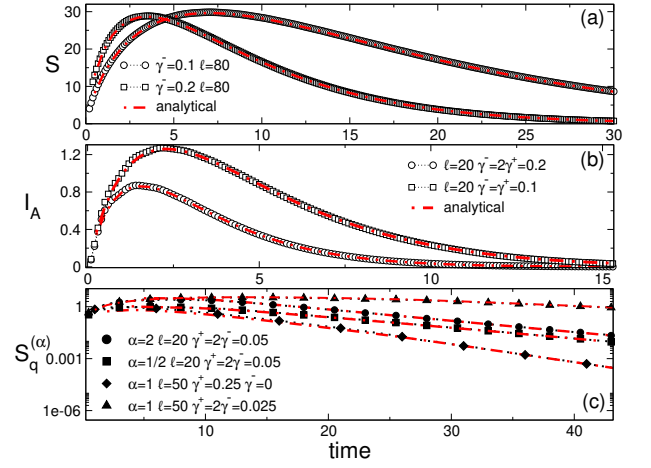


FIG. 2. Effect of gain/loss dissipation in the XX chain after the Néel quench. γ^\pm are dissipation rates. (a) Dynamics of the entropy S for $\gamma^+ = 0$. ℓ is the subsystem size. Symbols are exact numerical data. Dashed-dotted lines denote (13). (b) Dynamics of I_A . (c) Dynamics of S_q (cf. (11)). Now the dashed dotted lines denote the large t results (c.f. (12) (H19)).

relevant dissipation rate. Similar scaling persists for both incoherent hopping and dephasing, suggesting robustness of the quasiparticle picture to non-quadratic dissipative contributions.

Gain/loss dissipation.— For gain/loss dissipation the Lindblad generator (1) is quadratic. The ensuing dynamics maps Gaussian states onto Gaussian states. The system is thus completely characterized by its two-point correlation functions. Assuming that at $t = 0$ one has $\langle c_m c_n \rangle = 0$ and $\langle c_m \rangle = 0$, the relevant covariance matrix is $G_t \equiv \langle c_m^\dagger c_n \rangle_t$. The Rényi entropies are obtained from the eigenvalues λ_i of G_t restricted to A (cf. (4)) as [51] $S^{(\alpha)} = 1/(1-\alpha) \sum_i \ln[\lambda_i^\alpha + (1-\lambda_i)^\alpha]$. The time-evolved G_t is given by

$$G_t = e^{t\Lambda} G_0 e^{t\Lambda^\dagger} + \int_0^t dz e^{(t-z)\Lambda} \Gamma^+ e^{(t-z)\Lambda^\dagger}, \quad (3)$$

with $\Lambda = ih - 1/2(\Gamma^+ + \Gamma^-)$, where h is the Hamiltonian matrix, and $\Gamma_{mn}^\pm = \gamma^\pm \delta_{mn}$.

It is useful to introduce the unitarily-evolved correlation matrix $\tilde{G}_t = e^{iht} G_0 e^{-iht}$. Since Γ^\pm is diagonal, the eigenvalues λ_i of G_t are

$$\lambda_i = n_\infty(1 - b(t)) + \tilde{\lambda}_i b(t), \quad (4)$$

with $\tilde{\lambda}_i$ being the eigenvalues of \tilde{G}_t , and

$$n_\infty \equiv \frac{\gamma^+}{\gamma^+ + \gamma^-}, \quad b(t) \equiv e^{-(\gamma^+ + \gamma^-)t}. \quad (5)$$

Let us first consider a quench from the ferromagnet $|F\rangle \equiv |\downarrow\downarrow\cdots\rangle$, with homogeneous local fermionic occupation n_t . Physically, n_t satisfies the simple rate equation

$$dn_t = (1 - n_t)\gamma^+ dt - \gamma^- n_t dt. \quad (6)$$

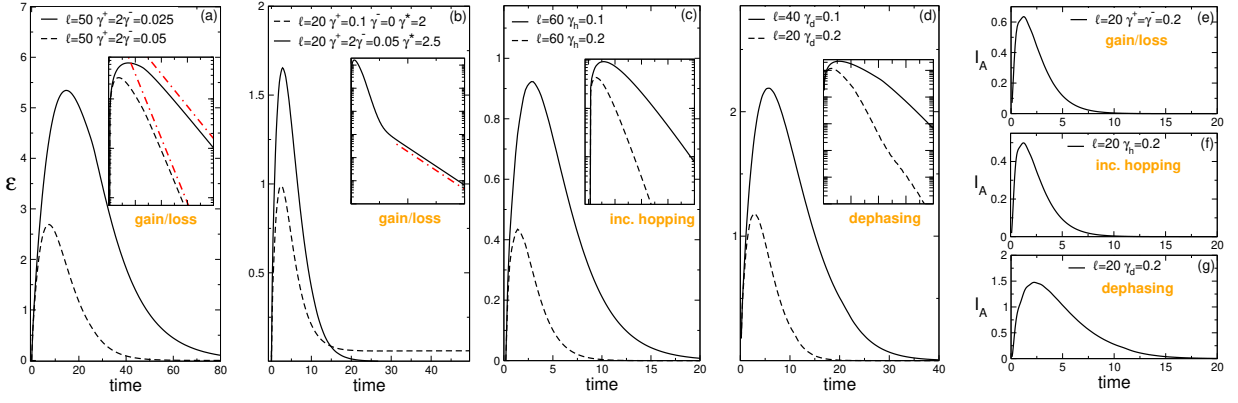


FIG. 3. Entanglement dynamics after the Néel quench in the XX chain with dissipation: diagonal gain/loss with rates γ^\pm (a), non-diagonal gain/loss with rates γ^\pm, γ^* (b), incoherent hopping with rate γ_h (c), and dephasing with rate γ_d (d). Panels (a-d) show \mathcal{E} . In all cases entanglement is created only up to $t \approx 1/\gamma$ with $\gamma = \gamma^\pm, \gamma_h, \gamma_d$. For diagonal gain/loss one has $\mathcal{E} \propto \exp(-2(\gamma^+ + \gamma^-)t)$ (dashed dotted line in the inset in (a)). In (b) the dashed-dotted line is $\mathcal{E} \propto \exp(-2(\gamma^- + \gamma^+)(\gamma - 2)t)$. Note that for $\gamma = 2$ the generator is gapless. Dissipation is off-diagonal resulting in a finite steady state value of \mathcal{E} . For incoherent hopping and dephasing \mathcal{E} decays at $t \ll \ell$. For $t \gg \ell$, i.e., in the steady state, \mathcal{E} attains a finite small value. (e-g) Mutual information I_A plotted as a function of time.

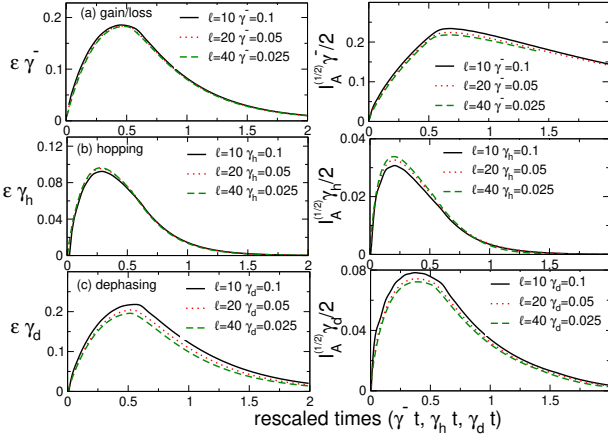


FIG. 4. Scaling behavior of \mathcal{E} and of $I_A^{(1/2)}$ (left and right column, respectively). Different panels are for different types of dissipation: gain/loss (a), incoherent hopping (b), and dephasing (c), with dissipation rates $\gamma^+, \gamma_h, \gamma_d$. The scaling limit is defined as $t, \ell, \rightarrow \infty, \gamma \rightarrow 0$, with t/ℓ and $\gamma\ell, \gamma t$ fixed.

Eq. (6) reflects that the probability to create a fermion in the interval $[t, t + dt]$ is $(1 - n_t)\gamma^+ dt$, whereas a fermion is removed with probability $n_t\gamma^- dt$. The solution of (6) is straightforward as

$$n_t = n_\infty \left\{ 1 - \left[(1 - n_0) - \frac{\gamma^-}{\gamma^+} n_0 \right] e^{-(\gamma^+ + \gamma^-)t} \right\}, \quad (7)$$

where n_0 is the initial occupation. Let us now consider the Néel state $|N\rangle \equiv |\uparrow\downarrow\uparrow\cdots\rangle$. Translational invariance is restored during the dynamics, and n_t is obtained by replacing n_0 with its average $\langle n_0 \rangle$ in Eq. (7). For the Néel state $\langle n_0 \rangle = 1/2$. The validity of Eq. (6) and (7) is numerically verified in Appendix B.

For open systems the Rényi entropies contain both in-

coherent and coherent contributions, where with coherent we mean those attributed to quasiparticles. As we shall see, a crucial role is played by the Yang-Yang entropies $S_{\text{cl}}^{(\alpha)}$, defined from n_t (cf. (7)) as

$$S_{\text{cl}}^{(\alpha)} = \frac{\ell}{1 - \alpha} \ln(n_t^\alpha + (1 - n_t)^\alpha), \quad (8)$$

where ℓ is the size of the portion of the chain considered. For $\alpha \rightarrow 1$ one obtains $S_{\text{cl}} = -\ell(n_t \ln n_t + (1 - n_t) \ln(1 - n_t))$. We now observe that for the quench from $|F\rangle$ the coherent contribution vanishes, as there are no quasiparticles. Thus Eq. (8) with $n_0 = 0$ (cf. Eq (7)) entirely determines the entropies (see Appendix B). This is different for the Néel state. We first consider the incoherent contribution. Within the quasiparticle picture this determines completely the full-system entropies, since the quasiparticles never leave the chain from its boundaries. Let us consider a quench from a product state obtained by translation of a unit cell with N_\uparrow up spins and N_\downarrow down spins. In the absence of dissipation the spectrum of G_t calculated over the full system is trivial at any time and it contains $N_\uparrow(N_\downarrow)$ eigenvalues 1(0). In the presence of dissipation the dynamics is described by the rate equation (6), implying that at time t , G_t has $N_\uparrow[N_\downarrow]$ eigenvalues $n_t(n_0 = 1)[n_t(n_0 = 0)]$. This implies that the full-system entropies are (see also Appendix B)

$$\langle S_{\text{cl}}^{(\alpha)} \rangle = \frac{N_\uparrow S_{\text{cl}}^{(\alpha)}(n_0 = 1) + N_\downarrow S_{\text{cl}}^{(\alpha)}(n_0 = 0)}{N_\downarrow + N_\uparrow}. \quad (9)$$

It is natural to wonder whether the entropy of the average $S_{\text{cl}}^{(\alpha)}(\langle n_0 \rangle)$ plays any role. Note that since the “melting” of the initial inhomogeneity happens because of coherent hopping, one should expect $S^{(\alpha)}(\langle n_0 \rangle)$ to give a coherent contribution. For the following it is useful to observe that $\langle S^{(\alpha)}(n_0) \rangle = S^{(\alpha)}(\langle n_0 \rangle)$ in the limit $t \rightarrow \infty$.

We now consider the entropies of a finite interval. To reveal the coherent contribution due to quasiparticles it is convenient to consider the large t limit of the von Neumann entropy. By using (4) we obtain

$$S = S_{\text{cl}}(t \rightarrow \infty) + \sum_i \left\{ 2b(\tilde{\lambda}_i - n_\infty) \text{atanh}(1 - 2n_\infty) + \frac{(n_\infty - \tilde{\lambda}_i)^2}{2n_\infty(n_\infty - 1)} b^2 + o(b^2) \right\}, \quad (10)$$

where $\tilde{\lambda}_i$ are introduced in (4). Eq. (10) can be simplified by using that $\sum_i \tilde{\lambda}_i = \langle n_0 \rangle \ell$. Interestingly, up to order $\mathcal{O}(b)$ Eq. (10) coincides with the large t expansion of $\langle S(n_0) \rangle$. This suggests to define the coherent part S_q as

$$S_q \equiv S - \langle S_{\text{cl}}(n_0) \rangle = \frac{e^{-2(\gamma^+ + \gamma^-)t}}{2n_\infty(n_\infty - 1)} \left[\sum_i \left(\frac{\tilde{\nu}_i^2 - 1}{4} \right) + \langle n_0 \rangle - \langle n_0^2 \rangle \right]. \quad (11)$$

Here we have $\tilde{\nu}_i \equiv 2\tilde{\lambda}_i - 1$. For an initial product state, which is also eigenstate of the total number operator, one has $n_0 - \langle n_0^2 \rangle = 0$. Eq. (11) depends on $\tilde{\lambda}_i$, suggesting that S_q is sensitive to coherent quasiparticle correlations, whereas the damping factor accounts for decoherence. We mention that a similar cancellation of the incoherent part as in (11) is encoded by construction in \mathcal{E} (see Appendix F), reflecting that the negativity is a genuine entanglement measure. To proceed, we observe that in free-fermion systems $\sum_i (\tilde{\nu}_i)^p$ can be calculated analytically [52] for any p (see Appendix H). For the Néel quench for $t \ll \ell$ one obtains

$$S_q \approx \frac{4t}{\pi} \frac{e^{-2(\gamma^+ + \gamma^-)t}}{n_\infty(1 - n_\infty)}. \quad (12)$$

A similar result for $S_q^{(\alpha)}$ is reported in Appendix H. Interestingly, Eq. (12) suggests that quasiparticles have finite lifetime $1/(\gamma^+ + \gamma^-)$, but this is not the only effect of dissipation. Indeed, the quasi-particle correlation content is not $\ln(2)$ as in the pure case. Remarkably, we can resum the large t expansion of Eq. (11) (see Appendix H). This yields

$$S^{(\alpha)} = \int \frac{d\lambda}{2\pi} \left[\max(1 - 2|v|t/\ell, 0) \langle S_{\text{cl}}^{(\alpha)}(n_0) \rangle + \min(2|v|t/\ell, 1) S_{\text{cl}}^{(\alpha)}(\langle n_0 \rangle) \right], \quad (13)$$

with $v(\lambda) = \sin(\lambda)$ the fermion velocity. Eq. (13) holds in the scaling limit $t, \ell \rightarrow \infty$, $\gamma^\pm \rightarrow 0$ with t/ℓ and $\gamma^\pm \ell$, γ^+/γ^- fixed, however, it is also quite accurate for moderately large γ^\pm and small ℓ . From (13), the scaling behavior (2) is apparent (note that $S_{\text{cl}} \propto \ell$). It is enlightening to consider the limit $v_{\text{max}} t/\ell < 1$. Clearly, Eq. (13) contains the incoherent contribution $\langle S_{\text{cl}}(n_0) \rangle$. Concomitantly, the term $\int d\lambda/(2\pi) |v|t [S_{\text{cl}}^{(\alpha)}(\langle n_0 \rangle) - \langle S_{\text{cl}}^{(\alpha)}(n_0) \rangle]$,

which coincides with S_q (cf. (11)), describes the coherent contribution due to quasiparticle pairs. Interestingly, the second term in the square brackets reveals how the environment suppresses the quasi-particle correlation. A striking consequence of (13) is that $I_A^{(\alpha)}$ is sensitive to the coherent term only. If A (cf. Fig. 1) is the semi-infinite chain, it is straightforward to check that $I_A^{(\alpha)} = 2S_q^{(\alpha)}$.

Eq. (13) exhibits an interesting behavior at short times $t \ll 1/\gamma^\pm$. It is easy to show that

$$\langle S_{\text{cl}}^{(\alpha)}(n_0) \rangle \rightarrow \begin{cases} \frac{\alpha}{2(\alpha-1)} t \ell (\gamma^+ + \gamma^-) & \alpha > 1 \\ \frac{t^\alpha \ell}{2(1-\alpha)} ((\gamma^+)^{\alpha} + (\gamma^-)^{\alpha}) & \alpha < 1 \\ -\frac{t\ell}{2} \sum_{a=\pm} \gamma^a (\ln t \gamma^a - 1) & \alpha = 1 \end{cases} \quad (14)$$

Crucially, $\langle S^{(\alpha)} \rangle$ vanishes for $\gamma^+, \gamma^- \rightarrow 0$, revealing its incoherent origin. Oppositely, one has $S^{(\alpha)}(\langle n_0 \rangle) \rightarrow \ell \ln 2$, as without dissipation. We notice that Eq. (14) predicts a non-linear growth with time for the entropy, even for $t \ll 1/\gamma^\pm$, in contrast with the random unitary scenario [53–57].

Numerical results.— We now provide some numerical results. In Fig. 2 (a) we focus on the von Neumann entropy. The dashed dotted lines denote (13), and are in perfect agreement with exact numerical data. The agreement is excellent already for $\ell = 20$, in contrast with the unitary case (see Ref. 2) where $t, \ell \rightarrow \infty$ is needed. In Fig. 2 (b) we discuss I_A . Again, already for $\ell = 20$ the numerical data are in spectacular agreement with theoretical predictions from Eq. (13). In Fig. 2 (c) we discuss the large t limit of $S_q^{(\alpha)}$ (cf. (11)). For all the values of α, γ^\pm, ℓ , the agreement with the theory is perfect.

We now discuss the negativity \mathcal{E} in Fig. 3. In Fig. 3 (a) we show \mathcal{E} for gain/loss dissipation. The behavior is qualitatively similar to that of I_A , with a non-linear increase up to $t \approx 1/(\gamma^+ + \gamma^-)$, followed by an exponential decay (see the inset) at long times. This reflects that the Liouvillian has a gap $\gamma^+ + \gamma^-$. In Fig. 3 (b) we consider the off-diagonal gain/loss matrices $\Gamma_{mn}^\pm = \gamma^\pm (\gamma^* \delta_{mn} + \delta_{m,n-1} + \delta_{m,n+1})$, where $\gamma^* \geq 2$. Now, the Liouvillian is gapless for $\gamma^* = 2$. Figure 3 shows that for $\gamma > 2$, \mathcal{E} decays exponentially as in (a). Surprisingly, for $\gamma^* = 2$, \mathcal{E} attains a finite, albeit small, value at $t \rightarrow \infty$. For $\gamma^* > 2$, the decay seems to be well described by $\mathcal{E} \propto \exp(-2(\gamma^+ + \gamma^-)(\gamma^* - 2)t)$.

In Fig. 3 (c-d) we consider incoherent hopping and dephasing, respectively, with rates γ_h, γ_d (see Appendix C D). The generator is no longer quadratic, although G_t can be obtained efficiently. Here we consider $S^{(\alpha)}$ and \mathcal{E} as defined from G_t , neglecting deviations from gaussian behavior. As it is clear from Fig. 3 (c-d), \mathcal{E} increases in a non-linear way up to $t \approx 1/\gamma$, and decreases for $t \rightarrow \infty$. In both cases \mathcal{E} attains a finite value $\mathcal{E} \approx 10^{-6}$ at $t \gg \ell$, which could be attributed to the existence of a metastable prestationary regime. Finally, in Fig. 3 (e-g) we show that the qualitative behavior of \mathcal{E} and I_A are similar.

A striking prediction of (13) is that $S^{(\alpha)}$ exhibits the scaling (2). This is inherited by $I_A^{(\alpha)}$. It is natural to

expect that the quasiparticle picture holds for \mathcal{E} . In Fig. 4 we compare $\gamma\mathcal{E}$ and $\gamma I_A^{(1/2)}/2$ plotted versus γt ($\gamma = \gamma^\pm, \gamma_h, \gamma_d$). Clear scaling behavior is visible in all cases. Crucially, the scaling functions describing \mathcal{E} and $I_A^{(1/2)}$ are different, unlike the unitary case (see Ref. 44).

Conclusions.— We have provided the first exact formulae describing information spreading in open quantum systems. There is an enormous scope for future research. First, there is the need to verify our results in different models and for different initial states. Second, our results lay the foundation for generalizations of the quasiparticle picture to dissipative interacting integrable models. This would allow to study the interplay

between interactions and dissipation [58] in the entanglement dynamics. Furthermore, it is extremely important to generalize (13) for the negativity. Finally, as observed, dissipation can serve to mitigate scaling corrections: this certainly deserves further investigation in numerical simulations and in experiments.

Acknowledgments.— We would like to thank Maurizio Fagotti for several useful discussions about the results of Ref. 52. V.A. acknowledges support from the European Research Council under ERC Advanced grant 743032 DYNAMINT. F.C. acknowledges support through a Teach@Tübingen Fellowship.

-
- [1] P. Calabrese and J. Cardy, Evolution of entanglement entropy in one-dimensional systems, *J. Stat. Mech.* (2005) P04010.
- [2] M. Fagotti and P. Calabrese, Evolution of entanglement entropy following a quantum quench: Analytic results for the XY chain in a transverse magnetic field, *Phys. Rev. A* **78**, 010306 (2008);
- [3] V. Alba and P. Calabrese, Entanglement and thermodynamics after a quantum quench in integrable systems, *PNAS* **114**, 7947 (2017).
- [4] S. Bose, Quantum communication through spin chain dynamics: an introductory overview, *Contemporary Physics*, **48**, 13 (2007).
- [5] A. Smith, M. S. Kim, F. Pollmann, and J. Knolle, Simulating quantum many-body dynamics on a current digital quantum computer, *npj Quantum Information* **5**, 106 (2019).
- [6] S. W. Hawking, Particle creation by black holes, *Comm. Math. Phys.* **43**, 199 (1975).
- [7] S. W. Hawking, Breakdown of predictability in gravitational collapse, *Phys. Rev. D* **14**, 2460 (1976).
- [8] P. Hayden and J. Preskill, Black holes as mirrors: quantum information in random subsystems, *JHEP*, **120** (2007).
- [9] D. N. Page, Average entropy of a subsystem, *Phys. Rev. Lett.* **71**, 1291 (1993).
- [10] D. N. Page, Information in black hole radiation, *Phys. Rev. Lett.* **71**, 3743 (1993).
- [11] N. Bao, S. M. Carroll, A. Chatwin-Davies, J. Pollack, and G. N. Remmen, Branches of the black hole wave function need not contain firewalls, *Phys. Rev. D* **97** (2018).
- [12] N. Bao, A. Chatwin-Davies, J. Pollack, and G. N. Remmen, Cosmological decoherence from thermal gravitons, [arXiv:1911.10207](https://arxiv.org/abs/1911.10207).
- [13] K. Agarwal and N. Bao, A toy model for decoherence in the black hole information problem, [arXiv:1912.09491](https://arxiv.org/abs/1912.09491).
- [14] H.-P. Breuer and F. Petruccione, *The Theory of Open Quantum Systems*, Ch. 3.5, p. 166, Oxford University Press, 2002.
- [15] S. Maity, S. Bandyopadhyay, S. Bhattacharjee, and A. Dutta, Growth of mutual information in a quenched one-dimensional open quantum manybody system, [arXiv:2001.09802](https://arxiv.org/abs/2001.09802).
- [16] V. Eisler, Crossover between ballistic and diffusive transport: The Quantum Exclusion Process, *J. Stat. Mech.* (2011), P06007.
- [17] J. Lee, M. S. Kim, Y. J. Park, and S. Lee, Partial teleportation of entanglement in a noisy environment, *J. Mod. Opt.* **47**, 2151 (2000).
- [18] G. Vidal and R. F. Werner, Computable Measure of Entanglement, *Phys. Rev. A* **65**, 032314 (2002).
- [19] J. Eisert and M. B. Plenio, A comparison of entanglement measures, *J. Mod. Opt.* **46**, 145 (1999).
- [20] M. B. Plenio, Logarithmic Negativity: A Full Entanglement Monotone That is not Convex, *Phys. Rev. Lett.* **95**, 090503 (2005); J. Eisert, Entanglement in quantum information theory, [quant-ph/0610253](https://arxiv.org/abs/quant-ph/0610253).
- [21] H. Wichterich, J. Molina-Vilaplana, and S. Bose, Scaling of entanglement between separated blocks in spin chains at criticality, *Phys. Rev. A* **80**, 010304 (2009).
- [22] S. Marcovitch, A. Retzker, M. B. Plenio, and B. Reznik, Critical and noncritical long-range entanglement in Klein-Gordon fields, *Phys. Rev. A* **80**, 012325 (2009).
- [23] P. Calabrese, J. Cardy, and E. Tonni, Entanglement Negativity in Quantum Field Theory, *Phys. Rev. Lett.* **109**, 130502 (2012).
- [24] P. Calabrese, J. Cardy, and E. Tonni, Entanglement negativity in extended quantum systems, *J. Stat. Mech.* (2013) P02008.
- [25] H. Shapourian, K. Shiozaki, and S. Ryu, Many-Body Topological Invariants for Fermionic Symmetry-Protected Topological Phases, *Phys. Rev. Lett.* **118**, 216402 (2017).
- [26] H. Shapourian, K. Shiozaki, and S. Ryu, Partial time-reversal transformation and entanglement negativity in fermionic systems, *Phys. Rev. B* **95**, 165101 (2017).
- [27] A. Coser, E. Tonni, and P. Calabrese, Entanglement negativity after a global quantum quench, *J. Stat. Mech.* (2014) P12017.
- [28] V. Eisler and Z. Zimboras, On the partial transpose of fermionic Gaussian states, *New J. Phys.* **17** 053048 (2015).
- [29] H. Shapourian and S. Ryu, Entanglement negativity of fermions: monotonicity, separability criterion and classification of few-mode states, [arXiv:1804.08637](https://arxiv.org/abs/1804.08637).
- [30] P. Calabrese, F. H. L. Essler, and G. Mussardo, Introduction to “Quantum Integrability in Out of Equilibrium Systems”, *J. Stat. Mech.* (2016) P064001.

- [31] F. H. L. Essler and M. Fagotti, Quench dynamics and relaxation in isolated integrable quantum spin chains, *J. Stat. Mech.* (2016) 064002.
- [32] L. Vidmar and M. Rigol, Generalized Gibbs ensemble in integrable lattice models, *J. Stat. Mech.* (2016) 64007.
- [33] J.-S. Caux, The Quench Action, *J. Stat. Mech.* (2016) 064006.
- [34] V. Alba and P. Calabrese, Entanglement dynamics after quantum quenches in generic integrable systems, *SciPost Phys.* **4**, 017 (2018).
- [35] V. Alba and P. Calabrese, Quench action and Rényi entropies in integrable systems, *Phys. Rev. B* **96**, 115421 (2017).
- [36] V. Alba and P. Calabrese, Rényi entropies after releasing the Néel state in the XXZ spin-chain, *J. Stat. Mech.* (2017), 113105.
- [37] M. Mestyán, V. Alba, and P. Calabrese, Rényi entropies of generic thermodynamic macrostates in integrable systems, *J. Stat. Mech.* 083104 (2018).
- [38] V. Alba, Towards a Generalized Hydrodynamics description of Rényi entropies in integrable systems, *Phys. Rev. B* **99**, 045150 (2019).
- [39] V. Alba and P. Calabrese, Quantum information scrambling after a quantum quench, *Phys. Rev. B* **100**, 115150 (2019).
- [40] V. Alba, Entanglement and quantum transport in integrable systems, *Phys. Rev. B* **97**, 245135 (2018).
- [41] B. Bertini, M. Fagotti, L. Piroli, and P. Calabrese, Entanglement evolution and generalised hydrodynamics: noninteracting systems, *J. Phys. A: Math. Theor.* **51**, 39LT01 (2018).
- [42] V. Alba, B. Bertini, and M. Fagotti, Entanglement evolution and generalised hydrodynamics: interacting integrable systems, *SciPost Phys.* **7**, 005 (2019).
- [43] M. Mestyán and V. Alba, Molecular dynamics simulation of entanglement spreading in generalized hydrodynamics, [arXiv:1905.03206](https://arxiv.org/abs/1905.03206).
- [44] V. Alba and P. Calabrese, Quantum information dynamics in multipartite integrable systems, *EPL* **126** 60001 (2019).
- [45] J. Kudler-Flam, Y. Kusuki, and S. Ryu, Correlation measures and the entanglement wedge cross-section after quantum quenches in two-dimensional conformal field theories, [arXiv:2001.05501](https://arxiv.org/abs/2001.05501).
- [46] M. Gruber and V. Eisler, Time evolution of entanglement negativity across a defect, [arXiv:2001.06274](https://arxiv.org/abs/2001.06274).
- [47] B. Bertini, E. Tartaglia, and P. Calabrese, Entanglement and diagonal entropies after a quench with no pair structure, *J. Stat. Mech.* 063104 (2018).
- [48] A. Bastianello and P. Calabrese, Spreading of entanglement and correlations after a quench with intertwined quasiparticles, *SciPostPhys* **5**, 033 (2018).
- [49] A. Bastianello and M. Collura, Entanglement spreading and quasiparticle picture beyond the pair structure, [arXiv:2001.01671](https://arxiv.org/abs/2001.01671).
- [50] T. Prosen, Third quantization: a general method to solve master equations for quadratic open Fermi systems, *New J. Phys.* **10** 043026 (2008).
- [51] I. Peschel and V. Eisler, Reduced density matrices and entanglement entropy in free lattice models, *J. Phys. A: Math. Theor.* **42**, 504003 (2009).
- [52] M. Fagotti, F. H. L. Essler, and P. Calabrese, Quantum Quench in the Transverse Field Ising chain I: Time evolution of order parameter correlators, *J. Stat. Mech.* (2012), P07016.
- [53] Y. Li, X. Chen and M. P. A. Fisher, Quantum Zeno effect and the many-body entanglement transition, *Phys. Rev. B* **98**, 205136 (2018).
- [54] B. Skinner, J. Ruhman, and A. Nahum, Measurement-Induced Phase Transitions in the Dynamics of Entanglement, *Phys. Rev. X* **9**, 031009.
- [55] C.-M. Jian, Y.-Z. You, R. Vasseur, and A. W. W. Ludwig, Measurement-induced criticality in random quantum circuits, [arXiv:1908.08051](https://arxiv.org/abs/1908.08051).
- [56] S. Choi, Y. Bao, X.-L. Qi, and E. Altman, Quantum Error Correction in Scrambling Dynamics and Measurement Induced Phase Transition, [arXiv:1903.05124](https://arxiv.org/abs/1903.05124).
- [57] X. Cao, A. Tilloy, and A. De Luca, Entanglement in a fermion chain under continuous monitoring, *SciPost Phys.* **7**, 024 (2019).
- [58] Z. Cai and T. Barthel, Algebraic versus Exponential Decoherence in Dissipative Many-Particle Systems, *Phys. Rev. Lett.* **111**, 150403 (2013).
- [59] P. Mazza, J.-M. Stéphan, E. Canovi, V. Alba, M. Brockmann, and M. Haque, Overlap distributions for quantum quenches in the anisotropic Heisenberg chain, *J. Stat. Mech.* (2016) P013104.

Appendix A: A simple proof of the scaling (2)

In this section we show that the scaling behavior (2)

$$\gamma\mathcal{E} = g(\gamma t, \gamma\ell) \quad (\text{A1})$$

can be derived by assuming that the quasiparticle picture holds and that the quasiparticles have a finite lifetime.

We focus on the negativity \mathcal{E} between subsystem A and the rest (see Fig. 1), considering the limit $L \rightarrow \infty$. Within the quasiparticle picture, the negativity is proportional to the number of quasiparticles that are shared between A and its complement. This implies that

$$\mathcal{E} = \int_0^\pi d\lambda \int_0^L dx \int_{x' \in A} dx' \int_{x'' \in \bar{A}} dx'' \left\{ e(\lambda)\delta(x' - x - v(-\lambda)t)\delta(x'' - x - v(\lambda)t) \right\}, \quad (\text{A2})$$

where x is the point from which the entangled pair is emitted, and λ is the quasimomentum. Note that we perform the integral over half of the Brillouin zone $\lambda \in [0, \pi]$. We define the two intervals as $A = [0, \ell]$ and $\bar{A} = [\ell + 1, L]$. Here $e(\lambda)$ is the contribution of the quasiparticles to the negativity. We can perform the integration over x' to obtain

$$\mathcal{E} = \int_0^\pi d\lambda \int_0^L dx \int_{x'' \in \bar{A}} dx'' \left\{ e(\lambda)\theta(x + v(-\lambda)t + \ell)\theta(\ell - x - v(-\lambda)t)\delta(x'' - x - v(\lambda)t) \right\}. \quad (\text{A3})$$

Here the term $\theta(x + v(-\lambda)t + \ell)$ takes into account that the quasiparticles can bounce on the origin and exit sub-

system A at later times. The integration over x'' gives

$$\mathcal{E} = \int_0^\pi d\lambda \int_0^L dx \left\{ e(\lambda) \theta(x - v(\lambda)t + \ell) \theta(\ell - x + v(\lambda)t) \times \theta(x + v(\lambda)t - \ell) \theta(L - x - v(\lambda)t) \right\}, \quad (\text{A4})$$

where we used that $v(\lambda) = -v(\lambda)$. We now assume that $L \rightarrow \infty$. This implies that $\theta(L - x - v(\lambda)t) = 1$ for any λ, t . Thus, the expression above becomes

$$\mathcal{E} = 2 \int_0^\pi d\lambda \min(v(\lambda)t, \ell) e(\lambda) \quad (\text{A5})$$

In the presence of the environment, we assume that the probability for a quasiparticle with quasimomentum λ to survive up to time t is $\exp(-\gamma t)$, with γ the relevant rate. The calculations leading to (A5) remain the same, the only modification is a multiplicative factor $\exp(-2\gamma t)$, which is the probability for both the members of the entangled pair to survive. Clearly, now (A5) satisfies the scaling (2).

Appendix B: Some numerical checks for gain/loss Lindbladians

In this section we provide some numerical checks of (7). We also discuss the theory prediction for the full-system von Neumann entropy S_T , which depends only on the incoherent contribution.

In Fig. 5 we compare Eq. (7) with exact numerical data obtained by using (3). In the top panel we consider the quench from the ferromagnetic state $|F\rangle$ in the XX chain. We also consider the quench from the Néel state (bottom panel). For $|F\rangle$ the initial correlation matrix is exactly zero, whereas for the Néel state it is given as $G_0 = (1 - (-1)^i)/2\delta_{ij}$. In both panels, the numerical data obtained from (3) are well described by (7). We note that for the quench from the Néel state and $\gamma^+ = 0.05$ there are oscillating corrections to (7), which disappear in the long-time limit. These signals that for small γ^\pm the system remain coherent for short times.

The behavior of the full-system entropy is checked in Fig. 6. The figure shows the density of entropy S_T/L of the full chain for the quenches from $|F\rangle$ and the Néel state. For $|F\rangle$ the von Neumann entropy is obtained by using (7), with $n_0 = 0$ in (8), whereas for the Néel state we used (9).

Appendix C: Two-point functions for incoherent hopping

In this section we review the approach to determine the two-point correlation function $G = \langle c_n^\dagger c_m \rangle$ in free-fermion systems. We follow Ref. 16.

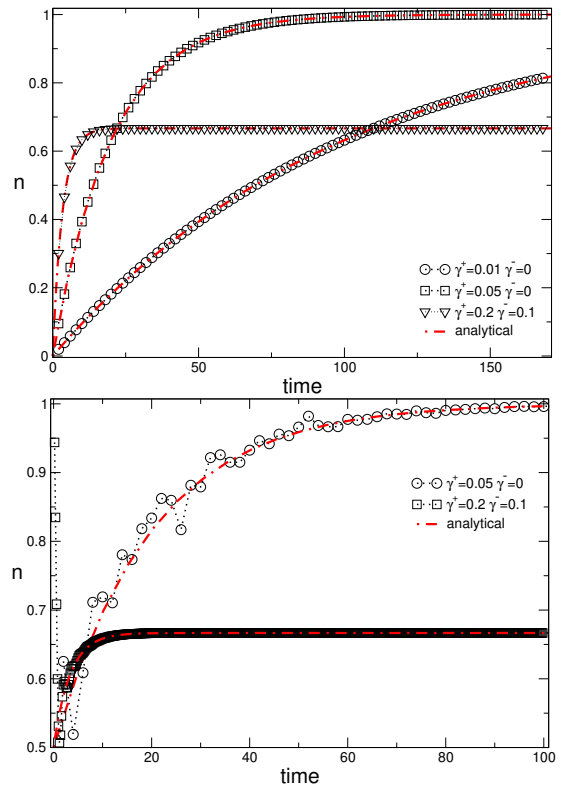


FIG. 5. Dynamics of the local density of fermions n in the XX chain in the presence of linear diagonal dissipation. (top) Results for the dynamics starting from the ferromagnetic state. (bottom) The same as in (top) for the quench from the Néel state. In both panels the symbols are exact numerical results, the dashed-dotted lines are the analytical results in (7). Note also that for $\gamma^+ = 0.05$ and $\gamma^- = 0$ strong oscillations are present for the Néel quench.

Let us consider Majorana fermions a_m as

$$a_{2m-1} = c_m + c_m^\dagger \quad (\text{C1})$$

$$a_{2m} = i(c_m - c_m^\dagger) \quad (\text{C2})$$

with anticommutation relations $\{a_k, a_l\} = 2\delta_{kl}$. We consider the generic Hamiltonian

$$H = \frac{i}{4} \sum_{k,l} H_{kl} a_k a_l, \quad H_{kl} = -H_{lk} \quad (\text{C3})$$

We also consider the generic Lindblad operator L_α

$$L_\alpha = \frac{i}{4} \sum_{k,l} L_{\alpha,kl} a_k a_l \quad (\text{C4})$$

It is important for the following to define a generic *ordered* string of Majorana operators Γ_ν as

$$\Gamma_\nu = a_1^{\nu_1} a_2^{\nu_2} \dots a_{2L}^{\nu_{2L}} \quad (\text{C5})$$

Here $\nu_i \in \{0, 1\}$ are the occupation numbers in the string.

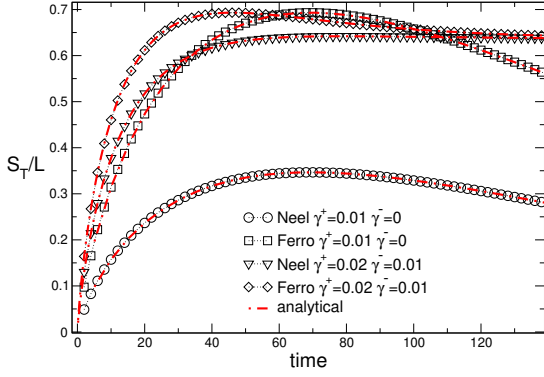


FIG. 6. Dynamics of the entanglement entropy of the full system in the presence of gain/loss. The system is the XX chain. The data are for the quench from the Néel state (circles and triangles) and the ferromagnetic state (diamonds and squares). The dashed dotted lines denote the analytical results obtained from (8) and (7).

We also define Majorana *superoperators* \hat{a}_j with action

$$\hat{a}_j \Gamma_{\underline{\nu}} = \delta_{1,\nu_j} \pi_j \Gamma_{\underline{\nu}'} \quad (\text{C6})$$

$$\hat{a}_j^\dagger \Gamma_{\underline{\nu}} = \delta_{0,\nu_j} \pi_j \Gamma_{\underline{\nu}'}', \quad (\text{C7})$$

where $\nu'_j = 1 - \nu_j$. The phase factor

$$\pi_j = \exp\left(i\pi \sum_{k=1}^{j-1} \nu_k\right) \quad (\text{C8})$$

ensures the fermionic anticommutation relations $\{\hat{a}_k, \hat{a}_l^\dagger\} = \delta_{kl}$. It is easy to prove that

$$[a_k a_l, \Gamma_{\underline{\nu}}] = 2(\hat{a}_k^\dagger \hat{a}_l - \hat{a}_l^\dagger \hat{a}_k) \Gamma_{\underline{\nu}} \quad (\text{C9})$$

For instance, the r.h.s. of (C9) becomes

$$2(-1)^{l-k} \pi_k \pi_l (\delta_{1,\nu_l} \delta_{0,\nu_k} \Gamma_{\underline{\nu}'} + \delta_{0,\nu_l} \delta_{1,\nu_k} \Gamma_{\underline{\nu}''}) \quad (\text{C10})$$

where $\nu'_l = 0 = 1 - \nu'_k$ and $\nu''_l = 1 = 1 - \nu''_k$. It is easy to check that if $\nu_l = \nu_k$ the term $a_k a_l$ commutes with $\Gamma_{\underline{\nu}}$. If $\nu_l \neq \nu_k$ one has that

$$a_k a_l \Gamma_{\underline{\nu}} = -\Gamma_{\underline{\nu}} a_k a_l, \quad (\text{C11})$$

which allows to prove (C9). By using (C9) one can derive the coherent part of the evolution as

$$i[H, \Gamma_{\underline{\nu}}] = - \sum_{k,l} H_{kl} \hat{a}_k^\dagger \hat{a}_l. \quad (\text{C12})$$

The incoherent contributions in (1) can be calculated as well. By using (C4) one obtains

$$\begin{aligned} \mathcal{L}_d(\Gamma_{\underline{\nu}}) \equiv & \frac{1}{16} \sum_{\alpha} \left(L_{\alpha}^{\dagger} \Gamma_{\underline{\nu}} L_{\alpha} - \frac{1}{2} \{ L_{\alpha}^{\dagger} L_{\alpha}, \Gamma_{\underline{\nu}} \} \right) = \\ & - \frac{1}{32} \sum_{\alpha,ijkl} \left(2L_{\alpha,ij} a_i a_j \Gamma_{\underline{\nu}} L_{\alpha,kl} a_k a_l \right. \\ & \left. - \{ L_{\alpha,ij} L_{\alpha,kl} a_i a_j a_k a_l, \Gamma_{\underline{\nu}} \} \right), \quad (\text{C13}) \end{aligned}$$

where we used that $L_{\alpha,ij} = -L_{\alpha,ji}$. Simple manipulations yield

$$\mathcal{L}_d(\Gamma_{\underline{\nu}}) = \frac{1}{32} \sum_{\alpha,ijkl} L_{\alpha,ij} L_{\alpha,kl} [a_i a_j, [a_k a_l, \Gamma_{\underline{\nu}}]]. \quad (\text{C14})$$

By applying (C9), one has

$$\mathcal{L}_d(\Gamma_{\underline{\nu}}) = \frac{1}{2} \sum_{\alpha,ijkl} L_{\alpha,ij} L_{\alpha,kl} \hat{a}_i^\dagger \hat{a}_j \hat{a}_k^\dagger \hat{a}_l \Gamma_{\underline{\nu}}. \quad (\text{C15})$$

By using that $L_{ij} = -L_{ji} = -L_{ij}^T$, and upon normal ordering, one obtains that the Liouvillian in (1) is given as

$$\mathcal{L} = - \sum_{kl} \tilde{H}_{kl} \hat{a}_k^\dagger \hat{a}_l + \frac{1}{2} \sum_{\alpha} \sum_{ijkl} L_{\alpha,ij}^T L_{\alpha,kl} \hat{a}_i^\dagger \hat{a}_k^\dagger \hat{a}_j \hat{a}_l, \quad (\text{C16})$$

where we defined \tilde{H}_{kl} as

$$\tilde{H}_{kl} = H_{kl} + \frac{1}{2} \sum_{\alpha} L_{\alpha,kl}^T L_{\alpha,kl}. \quad (\text{C17})$$

Let us now consider the XX hamiltonian. In terms of Majorana fermions one has

$$H_{kl} = -(\delta_{k,l-1} + \delta_{k,l+1}) \otimes \begin{pmatrix} 0 & -1 \\ 1 & 0 \end{pmatrix} \quad (\text{C18})$$

We choose the Lindbladians corresponding to incoherent hopping [16]

$$\begin{aligned} L_{2j-1,kl} = & \sqrt{\frac{\gamma \hbar}{2}} (\delta_{k,j} \delta_{l,j+1} \\ & + \delta_{k,j+1} \delta_{l,j}) \otimes \begin{pmatrix} 0 & -1 \\ 1 & 0 \end{pmatrix} \quad (\text{C19}) \end{aligned}$$

$$L_{2j,k,l} = \sqrt{\frac{\gamma \hbar}{2}} (\delta_{k,j} \delta_{l,j+1} - \delta_{k,j+1} \delta_{l,j}) \otimes \begin{pmatrix} 1 & 0 \\ 0 & 1 \end{pmatrix} \quad (\text{C20})$$

$$\frac{1}{2} \sum_{\alpha} L_{\alpha}^T L_{\alpha} = \delta_{kl} \otimes \begin{pmatrix} 1 & 0 \\ 0 & 1 \end{pmatrix} \quad (\text{C21})$$

It is convenient to work with the fermionic superoperators

$$\hat{a}_{-,m} = \frac{1}{\sqrt{2}} (\hat{a}_{2m-1} - i \hat{a}_{2m}), \quad (\text{C22})$$

$$\hat{a}_{+,m} = \frac{1}{\sqrt{2}} (\hat{a}_{2m-1} + i \hat{a}_{2m}) \quad (\text{C23})$$

which diagonalize the two-by-two matrix appearing in (C18) with eigenvalues $\pm i$. The inverse of (C22)(C23) is

$$\hat{a}_{2j-1} = \frac{1}{\sqrt{2}} (\hat{a}_{-,m} + \hat{a}_{+,m}), \quad (\text{C24})$$

$$\hat{a}_{2j} = \frac{i}{\sqrt{2}} (\hat{a}_{-,m} - \hat{a}_{+,m}). \quad (\text{C25})$$

Now, from (C16) one obtains

$$\mathcal{L} = \mathcal{L}_+ + \mathcal{L}_- + \mathcal{L}_{+-}. \quad (\text{C26})$$

Here we defined

$$\begin{aligned} \mathcal{L}_\pm = \sum_{m=1}^L & \left[i(\hat{a}_{\pm,m}^\dagger \hat{a}_{\pm,m+1} + \hat{a}_{\pm,m+1}^\dagger \hat{a}_{\pm,m}) - \gamma_h \hat{a}_{\pm,m}^\dagger \hat{a}_{\pm,m} \right. \\ & \left. + \gamma_h \hat{a}_{\pm,m}^\dagger \hat{a}_{\pm,m} \hat{a}_{\pm,m+1}^\dagger \hat{a}_{\pm,m+1} \right] \end{aligned} \quad (\text{C27})$$

$$\begin{aligned} \mathcal{L}_{+-} = \sum_{m=1}^L & \gamma_h \left[\hat{a}_{-,m}^\dagger \hat{a}_{-,m+1} \hat{a}_{+,m}^\dagger \hat{a}_{+,m+1} \right. \\ & \left. + \hat{a}_{+,m+1}^\dagger \hat{a}_{+,m} \hat{a}_{-,m+1}^\dagger \hat{a}_{-,m} \right] \end{aligned} \quad (\text{C28})$$

To proceed, one has to determine the action of the fermionic superoperators on a string of fermions. A simple calculation gives that the only nonzero combinations are

$$\hat{a}_{-,k} a_m^\dagger = \frac{1}{\sqrt{2}} \delta_{km} \quad (\text{C29})$$

$$\hat{a}_{+,k} a_m = \frac{1}{\sqrt{2}} \delta_{k,m} \quad (\text{C30})$$

$$\hat{a}_{-,k}^\dagger = \sqrt{2} a_k^\dagger \quad (\text{C31})$$

$$\hat{a}_{+,k}^\dagger = \sqrt{2} a_k. \quad (\text{C32})$$

Now one can derive the evolution of $G_{nm} = \langle a_n^\dagger a_m \rangle$ by using that

$$\frac{d}{dt} G_{kl} = \langle \mathcal{L}(a_k^\dagger a_l) \rangle. \quad (\text{C33})$$

One obtains the system of equations as

$$\begin{aligned} \frac{d}{dt} G_{kl} = & i(G_{k-1,l} + G_{k+1,l} - G_{k,l-1} - G_{k,l+1}) \\ & - 2\gamma_h G_{k,l} + \gamma_h \delta_{k,l} (G_{k-1,k-1} + G_{k+1,k+1}). \end{aligned} \quad (\text{C34})$$

1. The case of two qubits

It is interesting to study the logarithmic negativity of a two-qubits system. Here we consider the vectorized correlation matrix G_k . From (C34), the evolution of G_k is determined by

$$\frac{dG_k}{dt} = \sum_l M_{kl} G_l, \quad (\text{C35})$$

with the matrix M_{kl} given as

$$M_{kl} = \begin{pmatrix} -2\gamma_h & -i & i & 2\gamma_h \\ -i & -2\gamma_h & 0 & i \\ i & 0 & -2\gamma_h & -i \\ 2\gamma_h & i & -i & -2\gamma_h \end{pmatrix} \quad (\text{C36})$$

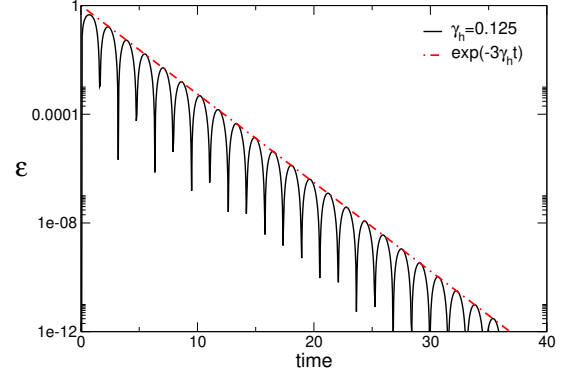


FIG. 7. Dynamics of the negativity between two spins in the XX chain with incoherent hopping with rate γ_h . The initial state is the Néel state. The continuous line denotes exact results. The dashed-dotted line is $\propto e^{-3\gamma_h t}$.

Note that M is complex and symmetric. The eigenvalues of M are given as

$$\lambda_0 = 0 \quad (\text{C37})$$

$$\lambda_1 = -2\gamma_h \quad (\text{C38})$$

$$\lambda_\pm = -3\gamma_h \pm \sqrt{\gamma_h^2 - 4} \quad (\text{C39})$$

with eigenvectors (not normalized)

$$v_0 = (1, 0, 0, 1) \quad (\text{C40})$$

$$v_1 = (0, 1, 1, 0) \quad (\text{C41})$$

$$\begin{aligned} v_- = & (-1, i(-\gamma_h + \sqrt{\gamma_h^2 - 4})/2, \\ & -i(-\gamma_h + \sqrt{\gamma_h^2 - 4})/2, 1) \end{aligned} \quad (\text{C42})$$

$$\begin{aligned} v_+ = & (-1, i(-\gamma_h - \sqrt{\gamma_h^2 - 4})/2, \\ & -i(-\gamma_h - \sqrt{\gamma_h^2 - 4})/2, 1) \end{aligned} \quad (\text{C43})$$

The matrix M is diagonalized as $D = U M U^T$ by the matrix $U_{ij} = \tilde{v}_{ij}$. The eigenvectors are normalized as $\tilde{v}_i = v_i / (\sum_j v_{ij}^2)^{1/2}$. The solution of (F5) is obtained

$$G(t) = \sum_l M_{kl}(t) G_l(0), \quad (\text{C44})$$

where

$$\begin{aligned} M(t) = & e^{\lambda_1 t} |\tilde{v}_1\rangle \langle \tilde{v}_1^*| + e^{\lambda_+ t} |\tilde{v}_+\rangle \langle \tilde{v}_+^*| \\ & + e^{\lambda_- t} |\tilde{v}_-\rangle \langle \tilde{v}_-^*|. \end{aligned} \quad (\text{C45})$$

To proceed one has to apply $M(t)$ to the vector with the initial correlations. From the time-evolved correlators it is straightforward to obtain the negativity associated

with the bipartition in which A is one of the two spins (see Appendix F).

There are several interesting observations. First, there is a regime for $\gamma_h < 2$ (weak incoherence) where quantum coherence to a certain extent survives. This is reflected in an oscillating behavior of \mathcal{E} with period $\pi/(4 - \gamma_h^2)^{1/2}$, superposed to an exponential decay. On the other hand, for $\gamma_h > 2$ (strong incoherence), the decay of \mathcal{E} is purely exponential. Finally, we should observe that the exponential decay is $\mathcal{E} \propto e^{-3\gamma_h t}$, and not $\mathcal{E} \propto e^{-2\gamma_h t}$, as one would have expected from (C38). This is because of the structure of the Néel state. This features are illustrated in Fig. 7.

Appendix D: Two-point function for dephasing

We now consider dephasing noise. Now the Lindblad operators are given as

$$L_{Lj} = L_{Rj} = \sqrt{\gamma_d} c_j^\dagger c_j \quad (\text{D1})$$

Note that the Lindbladian is hermitian, in contrast with the case of incoherent hopping. In terms of Majorana fermions one can write

$$\begin{aligned} \sqrt{\gamma_d} c_j^\dagger c_j &= \frac{\sqrt{\gamma_d}}{4} (a_{2j} a_{2j} + a_{2j-1} a_{2j-1} \\ &\quad - i a_{2j-1} a_{2j} + i a_{2j} a_{2j-1}). \end{aligned} \quad (\text{D2})$$

Therefore we can write the Lindblad operator

$$L_\alpha = \frac{i}{4} \sum_{k,l} L_{\alpha,kl} a_k a_l, \quad (\text{D3})$$

with

$$\begin{aligned} L_{2\alpha-1,kl} &= \sqrt{\gamma_d} (-i\delta_{k,2\alpha-1}\delta_{l,2\alpha-1} \\ &\quad - i\delta_{k,2\alpha}\delta_{l,2\alpha} - \delta_{k,2\alpha-1}\delta_{l,2\alpha} + \delta_{k,2\alpha}\delta_{l,2\alpha-1}) \end{aligned} \quad (\text{D4})$$

$$L_{2\alpha,kl} = 0. \quad (\text{D5})$$

Eq. (C14) holds for the dephasing as well. By using (C9), it is straightforward to obtain that

$$\begin{aligned} \mathcal{L}_d(\Gamma_\nu) &= \frac{1}{8} \sum_{ijkl} L_{\alpha,ij} L_{\alpha,kl} (\hat{a}_i^\dagger \hat{a}_j \hat{a}_k^\dagger \hat{a}_l - \hat{a}_i^\dagger \hat{c}_j \hat{a}_l^\dagger \hat{a}_k \\ &\quad - \hat{a}_j^\dagger \hat{a}_i \hat{a}_k^\dagger \hat{a}_l + \hat{a}_j^\dagger \hat{a}_i \hat{a}_l^\dagger \hat{a}_k) \Gamma_\nu. \end{aligned} \quad (\text{D6})$$

One can use that $L_{\alpha,lk} = -L_{\alpha,kl}^*$. This allows one to write

$$\begin{aligned} \mathcal{L}_d(\Gamma_\nu) &= \frac{1}{8} \sum_{ijkl} (L_{\alpha,ij} L_{\alpha,kl} + L_{\alpha,ij} L_{\alpha,kl}^* \\ &\quad + L_{\alpha,ij}^* L_{\alpha,kl} + L_{\alpha,ij}^* L_{\alpha,kl}^*) \hat{a}_i^\dagger \hat{a}_j \hat{a}_k^\dagger \hat{a}_l \end{aligned} \quad (\text{D7})$$

It is convenient to use the operators $\hat{a}_{\pm,m}$ defined in (C22) and (C23). Thus, Eq. (D7) becomes

$$\begin{aligned} \mathcal{L}_d(\Gamma_\nu) &= \frac{\gamma_d}{2} \sum_{m=1}^L (-\hat{a}_{-,m}^\dagger \hat{a}_{-,m} \hat{a}_{-,m}^\dagger \hat{a}_{-,m} \\ &\quad - \hat{a}_{+,m}^\dagger \hat{a}_{+,m} \hat{a}_{+,m}^\dagger \hat{a}_{+,m} + \hat{a}_{+,m}^\dagger \hat{a}_{+,m} \hat{a}_{-,m}^\dagger \hat{a}_{-,m} \\ &\quad + \hat{a}_{-,m}^\dagger \hat{a}_{-,m} \hat{a}_{+,m}^\dagger \hat{a}_{+,m}) \Gamma_\nu \end{aligned} \quad (\text{D8})$$

The expression above can be rewritten as

$$\begin{aligned} \mathcal{L}_d(\Gamma_\nu) &= \frac{\gamma_d}{2} \sum_{m=1}^L (-\hat{a}_{-,m}^\dagger \hat{a}_{-,m} - \hat{a}_{+,m}^\dagger \hat{a}_{+,m} \\ &\quad + 2\hat{a}_{+,m}^\dagger \hat{a}_{+,m} \hat{a}_{-,m}^\dagger \hat{a}_{-,m}) \Gamma_\nu \end{aligned} \quad (\text{D9})$$

Finally, the evolution of the two-point correlation in the presence of dephasing noise is given as

$$\begin{aligned} \frac{d}{dt} G_{kl} &= i(G_{k-1,l} + G_{k+1,l} - G_{k,l-1} - G_{k,l+1}) \\ &\quad - \gamma_d (G_{kl} - \delta_{kl} G_{kk}). \end{aligned} \quad (\text{D10})$$

As expected, the effect of the dephasing is to suppress off-diagonal correlations.

1. The case of two qubits

As for the case of incoherent hopping it is enlightening to consider the negativity in a two-qubits system. The evolution of the vectorized correlation matrix G_k is

$$\frac{d}{dt} G_k = \sum_l M_{kl} G_l. \quad (\text{D11})$$

Now the matrix M_{kl} reads as

$$M_{kl} = \begin{pmatrix} 0 & -i & i & 0 \\ -i & -\gamma & 0 & i \\ i & 0 & -\gamma & -i \\ 0 & i & -i & 0 \end{pmatrix} \quad (\text{D12})$$

The eigenvalues of M are given as

$$\lambda_0 = 0 \quad (\text{D13})$$

$$\lambda_1 = -\gamma \quad (\text{D14})$$

$$\lambda_\pm = (-\gamma \pm \sqrt{\gamma^2 - 16})/2 \quad (\text{D15})$$

with (not normalized) eigenvectors

$$v_0 = (1, 0, 0, 1) \quad (\text{D16})$$

$$v_1 = (0, 1, 1, 0) \quad (\text{D17})$$

$$\begin{aligned} v_- &= (-1, i(\gamma + \sqrt{\gamma^2 - 16})/4, \\ &\quad -i(\gamma + \sqrt{\gamma^2 - 16})/4, 1) \end{aligned} \quad (\text{D18})$$

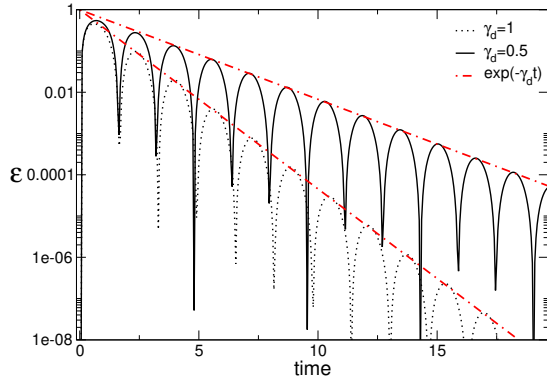


FIG. 8. Dynamics of the negativity \mathcal{E} between two spins in the XX chain with two sites in the presence of dephasing dissipation with rate γ_d . The initial state is the Néel state. The continuous lines are exact results. The dashed-dotted line is the behavior $e^{-\gamma_d t}$.

$$v_+ = (-1, i(\gamma - \sqrt{\gamma^2 - 16})/4, -i(\gamma - \sqrt{\gamma^2 - 16})/4, 1) \quad (\text{D19})$$

As for the case of incoherent hopping (see (C44)) the time-evolved correlation matrix is obtained from the matrix $M(t)$ given as

$$M(t) = e^{\lambda_1 t} |\tilde{v}_1\rangle \langle \tilde{v}_1^*| + e^{\lambda_+ t} |\tilde{v}_+\rangle \langle \tilde{v}_+^*| + e^{\lambda_- t} |\tilde{v}_-\rangle \langle \tilde{v}_-^*|, \quad (\text{D20})$$

where \tilde{v}_i are the normalized eigenvectors, as in (C45). Some qualitative features of the negativity \mathcal{E} is illustrated in Fig. 8. Now the negativity decays as $\mathcal{E} \propto e^{-\gamma_d t}$. Moreover, as for the incoherent hopping there are oscillations for $\gamma_d < 4$, whereas only exponential decay for $\gamma_d \geq 4$.

Appendix E: Additional data for incoherent hopping

Here we present some additional data for the behavior of the negativity \mathcal{E} in the XX chain in the presence of incoherent hopping. Specifically, here we show that in the long time regime $t \gg \ell$ with ℓ the size of subsystem A , \mathcal{E} attains a finite although small value.

Our data for several sizes ℓ of subsystem A and of the chain L are reported in Fig. 9. The figure shows both the negativity \mathcal{E} and the coherent contribution of the von Neumann entropy S_q (cf. (11)). The latter is obtained by subtracting from S the incoherent contribution (cf. (9)). Both \mathcal{E} and S_q exhibit a similar decay. As it is clear from the inset one has that $\mathcal{E}/S_q \approx 2$ for large times. We observe that both quantities attain a finite value at long times $t \gg \ell$. For instance, the data for $\ell = 20$ seem to saturate at $t \approx 10$ to a value 10^{-6} . Interestingly, the saturation happens later for larger values of $\ell = 40$.

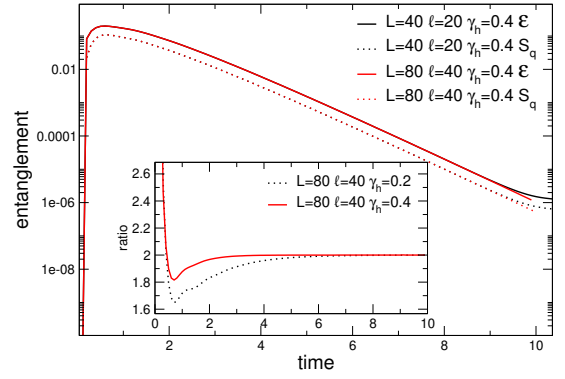


FIG. 9. Dynamics of the negativity \mathcal{E} after the quench from the Néel state in the XX in the presence of incoherent hopping with rate γ_h . The continuous lines denote the negativity, whereas the dotted lines are for S_q (cf. (11)). The inset show the ratio between the two. Note that at long times for $t \gg \ell$ both \mathcal{E} and S_q attain a finite small value 10^{-6} .

Appendix F: Fermionic logarithmic negativity

In this section we detail the calculation of the negativity \mathcal{E} introduced in Ref. 26 for free-fermion systems. To define \mathcal{E} , one introduces the fermionic correlation matrix G'_t as

$$G'_{mn} = \delta_{nm} - 2G_{nm}, \quad n, m = 1, \dots, L, \quad (\text{F1})$$

where G_{nm} is the same as in Eq. (3). Now, given a partition of the system as $A_1 \cup A_2$ (in Fig. 1 one has $A_1 = A$ and $A_2 = B$), one defines the matrices $G'_{11}, G'_{12}, G'_{21}, G'_{22}$ as

$$G' = \begin{pmatrix} G'_{11} & G'_{12} \\ G'_{21} & G'_{22} \end{pmatrix} \quad (\text{F2})$$

Here G'_{ij} with $i, j = 1, 2$ are obtained from G'_{nm} by requiring that $n \in A_i, m \in A_j$. One now defines the matrices G^\pm as

$$G^\pm = \begin{pmatrix} -G'_{11} & \pm i G'_{12} \\ \pm i G'_{21} & G'_{22} \end{pmatrix} \quad (\text{F3})$$

Now one defines the matrix P as

$$P \equiv \mathbb{I} + G^+ G^-, \quad (\text{F4})$$

where \mathbb{I} denotes the identity matrix. The key ingredient to define the fermionic negativity is the matrix G^T defined as

$$G^T \equiv \frac{1}{2} (\mathbb{I} - P^{-1} (G^+ + G^-)). \quad (\text{F5})$$

Given the eigenvalues ξ_i of G^T and the eigenvalues ζ_i of the covariance matrix G (see Eq. (3)), the fermionic negativity \mathcal{E} is defined as

$$\mathcal{E} = \sum_j \ln[\xi_j^{\frac{1}{2}} + (1 - \xi_j)^{\frac{1}{2}}] + \frac{1}{2} \sum_j \ln[\zeta_j^2 + (1 - \zeta_j)^2]. \quad (\text{F6})$$

1. Cancellation of the incoherent contributions

Here we show that in the presence of gain/loss dissipation the incoherent contribution cancels out in the definition of \mathcal{E} , at least up to order $\mathcal{O}(b)$, with $b \equiv e^{-(\gamma^+ + \gamma^-)t}$.

Let us define as \tilde{G} as the correlation matrix in the absence of dissipation (see the main manuscript). In the presence of gain/loss dissipation the matrix G' (cf. (F2)) is rewritten as

$$G' = (1 - 2n_\infty)(1 - b)\mathbb{I} + b\tilde{G}. \quad (\text{F7})$$

Here n_∞ is defined in (5). One now has the two matrices G^\pm (cf. (F3)) as

$$G^\pm = (1 - 2n_\infty) \begin{pmatrix} -\mathbb{I}_1 & 0 \\ 0 & \mathbb{I}_2 \end{pmatrix} - b(1 - 2a) \begin{pmatrix} -\mathbb{I}_1 & 0 \\ 0 & \mathbb{I}_2 \end{pmatrix} + b\tilde{G}^\pm. \quad (\text{F8})$$

Here \tilde{G}^\pm are obtained from (F3) after replacing $G'_{ij} \rightarrow \tilde{G}_{ij}$, with $i, j = 1, 2$. Here \mathbb{I}_i is the identity matrix restricted to subsystem A_i . It is convenient to separate the different powers of b . At the leading order in the limit $b \rightarrow 0$, i.e., $t \rightarrow \infty$, after using (F8) one has that the matrix P (cf. (F4)) is diagonal and it is given as

$$P = (1 + (1 - 2n_\infty)^2)\mathbb{I}. \quad (\text{F9})$$

The correlation matrix G^T (cf. (F5)) is also diagonal, and it is given as

$$G^T = \frac{1}{2} \begin{pmatrix} (1 + \frac{2(1-2n_\infty)}{1+(1-2n_\infty)^2})\mathbb{I}_1 & 0 \\ 0 & (1 - \frac{2(1-2n_\infty)}{1+(1-2n_\infty)^2})\mathbb{I}_2 \end{pmatrix} \quad (\text{F10})$$

At the leading order, the covariance matrix G (see (3)) is $n_\infty\mathbb{I}$. By using (F6), it is straightforward to show that the negativity vanishes in the steady state.

A similar cancellation occurs for the terms $\mathcal{O}(b)$. Up to first order $\mathcal{O}(b)$, P reads

$$P = (1 + (1 - 2b)(1 - 2n_\infty)^2)\mathbb{I} + 2b(1 - 2n_\infty) \begin{pmatrix} \tilde{G}_{11} & i\tilde{G}_{12} \\ -i\tilde{G}_{21} & \tilde{G}_{22} \end{pmatrix} \quad (\text{F11})$$

After keeping only the terms $\mathcal{O}(b)$, its inverse P^{-1} reads

$$P^{-1} = \frac{1}{1 + (1 - 2n_\infty)^2} \left[\left(1 + \frac{2b(1 - 2n_\infty)^2}{1 + (1 - 2n_\infty)^2} \right) \mathbb{I} - \frac{2b(1 - 2n_\infty)}{1 + (1 - 2n_\infty)^2} \begin{pmatrix} \tilde{G}_{11} & i\tilde{G}_{12} \\ -i\tilde{G}_{21} & \tilde{G}_{22} \end{pmatrix} \right] \quad (\text{F12})$$

Up to terms $\mathcal{O}(b)$, the matrix G^T reads

$$G^T = \frac{1}{2}\mathbb{I} - \frac{1}{2 + 2(1 - 2n_\infty)^2} \left[2(1 - 2n_\infty) \begin{pmatrix} -\mathbb{I}_1 & 0 \\ 0 & \mathbb{I}_2 \end{pmatrix} - 2b(1 - 2n_\infty) \begin{pmatrix} -\mathbb{I}_1 & 0 \\ 0 & \mathbb{I}_2 \end{pmatrix} + b\tilde{G}^+ + \tilde{b}G^- \right. \\ \left. + \frac{4b(1 - 2n_\infty)^3}{1 + (1 - 2n_\infty)^2} \begin{pmatrix} -\mathbb{I}_1 & 0 \\ 0 & \mathbb{I}_2 \end{pmatrix} - \frac{4b(1 - 2n_\infty)^2}{1 + (1 - 2n_\infty)^2} \tilde{G}^+ \right]. \quad (\text{F13})$$

We now use that the covariance matrix G is

$$G = n_\infty(1 - b)\mathbb{I} + \frac{b}{2}(\mathbb{I} - \tilde{G}) \quad (\text{F14})$$

To proceed, one has to substitute (F14) and (F13) in (F6), keeping only the terms $\mathcal{O}(b)$. A straightforward, although tedious, calculation gives that at $\mathcal{O}(b)$ the negativity vanishes.

Appendix G: Effect of the pair destruction

In this section we provide some further evidence for the validity of the quasiparticles picture for the negativity for the different sources of dissipation analyzed in the manuscript. The idea is to consider an inhomogeneous dissipation. Specifically, here we consider the case in which the Lindbladian acts only on the B part of the chain (see Fig. 1). Moreover, we consider the quench from an inhomogeneous initial state. Specifically, we prepare subsystem A in the Néel state, whereas part B is prepared in the ferromagnetic state. The physical picture is the following. Genuine quantum correlations, which are due to the creation of entangled pairs, are generated in A . As the quasiparticles travel, they entangle A and B . However, the presence of the Lindbladian on part B is expected to suppress the negativity, because it destroys one member of the entangled pair, implying that the entanglement decays.

This is explicitly checked in Fig. 10 for the case of diagonal dissipation (a), incoherent hopping (b), and dephasing (c). The figure shows \mathcal{E} for a chain of $L = 20$ sites. Subsystem A is the half-chain prepared in the ferromagnetic state. For each value of γ^\pm , γ_h and γ_d the negativity exhibits a plateau at $t \ll \ell$. The height of the plateaux decays in the limit of large dissipation.

Appendix H: Trace formulas for free fermion quenches

In this section we review the calculation of arbitrary traces of the correlation matrix after a quench in free-fermion models. We follow closely Ref. 52.

First, given the free-fermion creation and annihilation operators c_j^\dagger, c_j acting on site j , let us define the Majorana operators a_j^x, a_j^y as

$$a_j^x \equiv c_j^\dagger + c_j, \quad a_j^y \equiv i(c_j - c_j^\dagger). \quad (\text{H1})$$

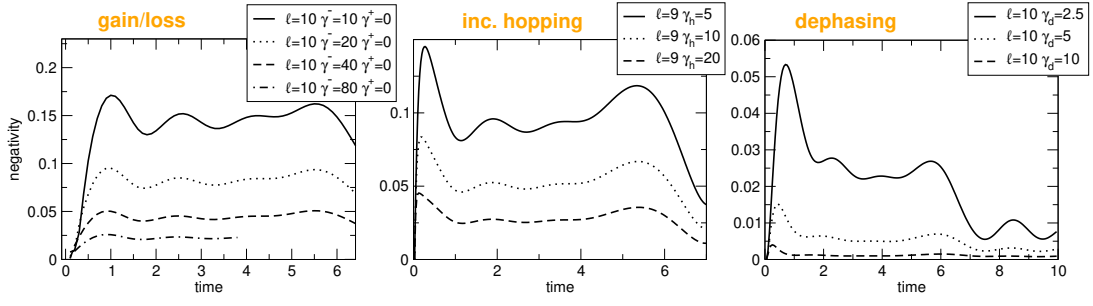


FIG. 10. Dynamics of the fermionic negativity \mathcal{E} in the XX chain in the presence of dissipation: pump/loss of particles (a), incoherent hopping (b), and dephasing (c). To measure the effect of the breaking of the pair structure, the dissipation is present only in the B part of the chain (see Fig. 1). Note that the negativity plateaux decay as $1/\gamma^-$ and $1/\gamma_h$, whereas for the dephasing the decay is faster as $1/\gamma_d^2$.

Let us define the matrix Γ as

$$\Gamma_{nm} = \begin{bmatrix} \delta_{mn} - \langle a_n^x a_m^x \rangle & -\langle a_n^x a_m^y \rangle \\ -\langle a_n^y a_m^x \rangle & \delta_{mn} - \langle a_n^y a_m^y \rangle \end{bmatrix}. \quad (\text{H2})$$

The matrix Γ is antisymmetric and has eigenvalues $\pm\nu_j$. This are related to the eigenvalues λ_j of the fermionic correlation matrix $G_{nm} \equiv \langle c_n^\dagger c_m \rangle$ as

$$\nu_j = 2\lambda_j - 1. \quad (\text{H3})$$

The matrix Γ is a 2 by 2 block Toeplitz matrix as

$$\Gamma = \begin{bmatrix} \Gamma_0 & \Gamma_{-1} & \cdots & \Gamma_{1-\ell} \\ \Gamma_1 & \Gamma_0 & & \vdots \\ \vdots & & \ddots & \vdots \\ \Gamma_{\ell-1} & \cdots & \cdots & \Gamma_0 \end{bmatrix}, \quad \Gamma_l = \begin{pmatrix} -f_l & g_l \\ -g_{-l} & f_l \end{pmatrix}, \quad (\text{H4})$$

with f_l, g_l some functions. The so-called block symbol $\hat{\Gamma}(k)$ is defined as the Fourier transform

$$\Gamma_l = \begin{pmatrix} -f_l & g_l \\ -g_{-l} & f_l \end{pmatrix} = \int_{-\pi}^{\pi} \frac{dk}{2\pi} e^{ikl} \hat{\Gamma}(k), \quad (\text{H5})$$

with $\hat{\Gamma}(k) = \begin{pmatrix} -f(k) & g(k) \\ -g(-k) & f(k) \end{pmatrix},$

Let us assume that $\hat{\Gamma}(k)$ can be parametrized as

$$\hat{\Gamma}(k) = n_x(k) \sigma_x^{(k)} + \vec{n}_\perp(k) \cdot \vec{\sigma}^{(k)} e^{2\epsilon(k)t \sigma_x^{(k)}}, \quad (\text{H6})$$

with $\vec{n}_\perp(k) \cdot \hat{x} = 0.$

Here $\sigma_{x,y,z}$ are Pauli matrices, $n_x \in \mathbb{R}$, t a real parameter, and \vec{n}_\perp an arbitrary three-dimensional vector. In (H6) $\epsilon(k)$ is an arbitrary function, although later we will identify it with the single-particle energy of the free-fermion Hamiltonian. We also define $\sigma_\alpha^{(k)}$ as

$$\sigma_\alpha^{(k)} \sim e^{i\vec{w}(k) \cdot \vec{\sigma}} \sigma_\alpha e^{-i\vec{w}(k) \cdot \vec{\sigma}}, \quad (\text{H7})$$

and the vector $\vec{w}(k)$ can be arbitrary. The main result is

that

$$\lim_{\substack{t, \ell \rightarrow \infty \\ t/\ell \text{ fixed}}} \frac{\text{Tr}[\Gamma^{2\beta}]}{2\ell} = \int_{-\pi}^{\pi} \frac{dk_0}{2\pi} \max\left(1 - 2|\epsilon'(k_0)| \frac{t}{\ell}, 0\right) \left(n_x(k_0)^2 + |\vec{n}_\perp(k_0)|^2\right)^{2\beta} + \int_{-\pi}^{\pi} \frac{dk_0}{2\pi} \min\left(2|\epsilon'(k_0)| \frac{t}{\ell}, 1\right) n_x(k_0)^{2\beta}. \quad (\text{H8})$$

Here $\epsilon'(k_0)$ is the derivative of ϵ . To use (H8) we notice that given the symbol of the initial correlation matrices $\hat{\Gamma}_0$, at generic time t one has

$$\hat{\Gamma}_t(k) = e^{-ih(k)t} \hat{\Gamma}_0 e^{ih(k)t}, \quad (\text{H9})$$

where $h(k)$ is the symbol of the free-fermion Hamiltonian generating the dynamics.

Importantly, the results above are valid for quenches from translationally invariant initial states. Here we are interested in the quench from the Néel state, which is not translational invariant. However, it is possible to restore translational invariance in the initial state by performing the simple unitary transformation U

$$U = \prod_{\text{even } j} \sigma_{x,j}. \quad (\text{H10})$$

Note that U is product of local unitary transformations, which implies that it does not affect the entanglement properties of the system. Clearly, U maps the Néel state in the ferromagnet $|\mathbb{F}\rangle$.

Here we are interested in quenches in the XX chain, which is defined by the Hamiltonian

$$H = \sum_j (\sigma_{x,j} \sigma_{x,j+1} + \sigma_{y,j} \sigma_{y,j+1}). \quad (\text{H11})$$

Under application of U , the XX chain is mapped to

$$H = \sum_j (\sigma_{x,j} \sigma_{x,j+1} - \sigma_{y,j} \sigma_{y,j+1}). \quad (\text{H12})$$

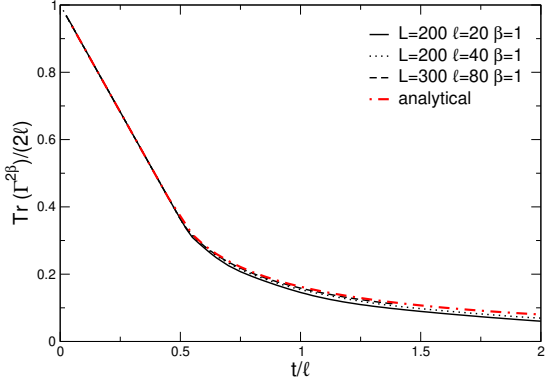


FIG. 11. Check of formula (H18) for the XX chain and the quench from the Néel state.

This corresponds to the XY chain in the limit of infinite anisotropy. Eq. (H11) is diagonalized by a Fourier transform. One obtains the single particle dispersion as

$$\epsilon(k) = \sin k. \quad (\text{H13})$$

The symbol $h(k)$ of the Hamiltonian above is

$$h(k) = \sin k \sigma_x. \quad (\text{H14})$$

Before applying (H8) we need to determine the evolved symbol $\hat{\Gamma}$ of the correlation matrix. For the ferromagnet $|F\rangle$, a straightforward calculation gives

$$\Gamma = \delta_{nm} \sigma_y. \quad (\text{H15})$$

Now the the symbol of the evolved correlation matrix $\hat{\Gamma}_t$ at time t reads as

$$\hat{\Gamma}_t \equiv e^{-ih(k)t} \sigma_y e^{ih(k)t} = e^{-i \sin(k) \sigma_x} \sigma_y e^{i \sin(k) \sigma_x}. \quad (\text{H16})$$

This is of the form in Eq. (H6) with

$$\vec{w} = (\sin(k), 0, 0), \quad n_x = 0, \quad \vec{n}_\perp = (0, 1, 0). \quad (\text{H17})$$

It is now straightforward to apply (H8). The integration over k_0 can be performed analytically, and one obtains that

$$\begin{aligned} \frac{\text{Tr}(\Gamma^{2\beta})}{2\ell} &= \left(1 - \frac{4}{\pi}\right) \frac{t}{\ell} \theta(\ell - 2t) \\ &+ \frac{2}{\pi} \left[-2\frac{t}{\ell} + \sqrt{\frac{4t^2}{\ell^2} - 1} + \text{arccsc}\left(\frac{2t}{\ell}\right) \right] \theta(2t - \ell). \end{aligned} \quad (\text{H18})$$

The result does not depend on the index β . This is a feature of the Néel state, and it can be derived by observing that the overlaps between the Néel state and the eigenstates of the XX chain are all equal [59].

In Fig. 11 we check the validity of Eq. (H8). Clearly, although scaling corrections are present, upon increasing t, ℓ , one recovers (H8). It is now clear that by using the large t expansion in (11) and (H18), it is straightforward to prove (12). Finally, a similar calculation yields the coherent contribution to the Rényi entropies $S_q^{(\alpha)}$ as

$$S_q^{(\alpha)} \approx \frac{-\alpha t e^{-2(\gamma^+ + \gamma^-)t}}{2\pi(1-\alpha)n_\infty^2(n_\infty - 1)^2((1-n_\infty)^\alpha + n_\infty^\alpha)^2} \times ((1-n_\infty)^\alpha n_\infty + (n_\infty - 1)n_\infty^\alpha)^2 - n_\infty^\alpha(1-n_\infty)^\alpha(\alpha - 1) \quad (\text{H19})$$

1. Resummation formula

Formula (H8) allows to obtain the behavior of arbitrary functions of Γ in the scaling limit. Precisely, let us consider

$$\text{Tr} \mathcal{F}(\Gamma^2) = \sum_\beta \mathcal{F}_\beta \text{Tr}(\Gamma^{2\beta}), \quad (\text{H20})$$

where we assumed that $\mathcal{F}(z)$ is an analytic function of z with power series expansion $\mathcal{F} = \sum_\beta \mathcal{F}_\beta z^\beta$ around $z = 0$. Now, one can use (H8), interchange the order of summation and integration, to obtain

$$\begin{aligned} \lim_{\substack{t, \ell \rightarrow \infty \\ t/\ell \text{ fixed}}} \frac{\text{Tr}[\mathcal{F}(\Gamma^2)]}{2\ell} &= \\ \int_{-\pi}^{\pi} \frac{dk_0}{2\pi} \max\left(1 - 2|\epsilon'(k_0)|\frac{t}{\ell}, 0\right) \mathcal{F}(n_x(k_0)^2 + |\vec{n}_\perp(k_0)|^2) \\ &+ \int_{-\pi}^{\pi} \frac{dk_0}{2\pi} \min\left(2|\epsilon'(k_0)|\frac{t}{\ell}, 1\right) \mathcal{F}(n_x(k_0)^2). \end{aligned}$$

Before applying this result to our problem, it is crucial to observe that for generic values of the gain/loss rate γ^\pm , due to the structure of the eigenvalues λ_i (cf. (4)), the entropies $S^{(\alpha)}$ are not even functions of the unitarily evolved eigenvalues $\tilde{\nu}_j$. Fortunately, this does not happen in the balanced gain/loss case, i.e., for $\gamma^+ = \gamma^-$. Then one has that the function $\mathcal{F}(z)$ is given as

$$\begin{aligned} \mathcal{F}(z) &= -\frac{1}{2}(1 - e^{-(\gamma^+ + \gamma^-)t} z) \ln \frac{1}{2}(1 - e^{-(\gamma^+ + \gamma^-)t} z) \\ &- \frac{1}{2}(1 + e^{-(\gamma^+ + \gamma^-)t} z) \ln \frac{1}{2}(1 + e^{-(\gamma^+ + \gamma^-)t} z), \end{aligned} \quad (\text{H21})$$

where $\gamma^+ = \gamma^-$. A straightforward calculation using (H21) gives (13). As it is shown in the main manuscript, although here we proved (13) for $\gamma^+ = \gamma^-$, we checked that it holds for arbitrary γ^\pm .